On the Topology of the Electron Charge Density at the Bond Critical Point of the Electron−Pair Bond

ARTICLE *in* THE JOURNAL OF PHYSICAL CHEMISTRY A · OCTOBER 1998

Impact Factor: 2.69 · DOI: 10.1021/jp981523k

2 AUTHORS, INCLUDING:

Luis Rincon
University of the Andes (Venezuela)
72 PUBLICATIONS **551** CITATIONS

On the Topology of the Electron Charge Density at the Bond Critical Point of the Electron-Pair Bond

Luis Rincón[†] and Rafael Almeida*

Departamento de Química, Facultad de Ciencias, Universidad de Los Andes, Mérida-5101, Venezuela

Received: March 17, 1998; In Final Form: August 5, 1998

Using the classical valence bond description of the electron-pair bond, as a resonance between a covalent structure and two ionic structures, we study the change in the topology of the charge density at the bond critical point. In the first part of this paper, the density of the H−H and Li−H bonds is analyzed in terms of three types of contributions: $\rho(A-B) = \rho_{cov} + \rho_{res} + \rho_{ion}$, the first contribution is due to the covalent structure, the second to the resonance between covalent and ionic structures, and the last one comes from the ionic structures. From this analysis, we conclude that when the bond is described as a covalent and one ionic structure, as in Li−H, the increase in the ionicity of the bond also corresponds with an increase in the closed-shell character of the electron density. However, in the case of the H−H bond, where the two ionic structures are equally important, the increment in the shared type interaction is due to the resonance between covalent and ionic structures. In the second part of this paper, we report an analysis of the classical valence bond description and the topological properties of the electron charge density calculated from *ab initio* GVB calculations for 15 different diatomic molecules at the equilibrium geometry and their dependence with the internuclear distance for H_2, LiH, F_2, Cl_2, Li_2, and Na_2 molecules. This analysis reveals the importance of the overlap between the hybrid orbitals in a Heitler−London type wave function in determining the topological properties at the bond-critical point for covalent bonding. For Li_2 we have found that at the equilibrium distance, the topology of ρ shows a maximum located at the middle of its bond, while for Cl_2 a similar maximum is found at shorter internuclear distances.

I. Introduction

In one of the first studies on the nature of the chemical bond, Linus Pauling proposed that the electron-pair bond could be described as a resonating state between one covalent and two ionic structures.[1] This idea is deeply rooted in the electron-pair description proposed by Lewis in 1916.[2] Employing the language of quantum mechanics, the resonant state involved in this idea is described by the wave function

$$\psi(A-B) = C_1\Phi(A\cdot\cdot B) + C_2\Phi(A^-B^+) + C_3\Phi(A^+B-) \quad (1)$$

in which the wave function $\Phi(A\cdot\cdot B)$ represents the covalent structure, and the two ionic structures are represented by $\Phi(A^-B^+)$ and $\Phi(A^+B^-)$. The relative values of the mixing coefficients, C_1-C_3, besides indicating the contribution of each structure to the total state, allow one to classify a bond anywhere in the range between "pure covalent" and "pure ionic". This *ansatz* wave function establishes a clear link between the intuitive valence bond (VB) description of the electron-pair bond and its associated molecular properties, such as the electron charge density.

On the other hand, in Bader's theory of *Atoms in Molecules*,[3] which is a theory of chemical structure and reactivity based on the topological properties of the electron charge density, ρ, the formation of a chemical bond is the result of a competition between the perpendicular contractions of ρ toward the bond path, which lead to a concentration of the charge density along this line and the parallel expansion of ρ away from the interatomic surface, which leads to its separate concentration in each atomic basin. This behavior results in the formation of a critical point in the charge density (bond critical point, hereafter called BCP), at which the Hessian of ρ has two negative eigenvalues (λ_1 and λ_2) and one positive eigenvalue (λ_3). This means that ρ exhibits two negative curvatures (λ_1 and λ_2) perpendicular to the interatomic line and one positive curvature (λ_3) along the interatomic line. Notice that for linear molecules in a $^1\Sigma$ (or $^1\Sigma_g$) state, such as the ones studied here, $\lambda_1 = \lambda_2$. In this theory, the atomic interactions are classified between two limiting behaviors: the shared and the closed-shell interactions. The shared interactions are characteristic of covalent and polar bonds. In this limiting situation, the charge distribution at the BCP is dominated by the perpendicular negative curvatures of the electron density. These shared interactions are characterized by large values of ρ, $\nabla^2\rho < 0$, and $|\lambda_1|/\lambda_3 > 1$ at the BCP. In contrast, for the closed-shell interactions, characteristic of ionic bonds, hydrogen bonds, and van der Waals molecules, the value of ρ is small, $\nabla^2\rho > 0$ and $|\lambda_1|/\lambda_3 \ll 1$. These behaviors can be better understood, if we recall that the local form of the virial theorem can be written as[3]

$$\frac{\hbar^2}{4m}\nabla^2\rho = 2G(\mathbf{r}) + V(\mathbf{r}) \quad (2)$$

where $G(\mathbf{r}) > 0$ is the electronic kinetic energy density and $V(\mathbf{r}) < 0$ is the electronic potential energy density, defined as the virial of the forces exerted on the electrons. Thus, the sign of $\nabla^2\rho$ serves to summarize the essential physical characteristics

* To whom correspondence should be addressed.
[†] Centro Nacional de Cálculo Cientifico (CeCalCULA), Parque Tecnologico de Mérida, Mérida-Venezuela.-

10.1021/jp981523k CCC: $15.00
Published on Web 10/27/1998

of the interactions which create the BCP. For the closed-shell interactions the kinetic energy density is the dominant contribution at the BCP, while for the shared interactions the potential energy density makes the prevailing contribution. Bader's classification has been tested in many well-defined sets of molecules, at least at the Hartree−Fock level.[3] This interpretation of the chemical bond is, in general, simple and satisfactory. In addition, when scanning among many chemical bonds, we observed that one may pass from one extreme behavior to another, not by a sudden and discontinuous change but, instead, by small gradations. Thus, it has been found that some bonds represent an intermediate situation between shared and closed shells systems. In these cases the BCP is located near the nodal region where $\nabla^2\rho = 0$. This topological partition, scheme of Bader has been extended to deal with VB wave functions contructed directly from nonorthogonal orbitals.[4,5] In those works, the authors reported results based on employing spin-coupled wave functions.[6]

Although the presence of the BCP in the internuclear bond path is a general result for most molecules, there are some exceptions. The most known example is the Li_2 molecule, which at the equilibrium geometry presents a maximum of ρ in the center of the Li−Li bond. This maximum of the density (a non-nuclear attractor) has been investigated in detail recently;[7−12] however, a conclusive explanation of its origin still remains to be given. A similar non-nuclear attractor has been reported for the Na_2 molecule by Gao et al.;[8] however, another study by Edgecombe et al.[11] has shown that high-quality basis sets remove the non-nuclear attractor in this molecule. At this moment, the non-nuclear attractor in Li_2 is always found, disregarding the level of complexity of the calculations and the basis sets employed.

Recently several methodologies, aiming to developing a more rigorous and quantitative classification of the chemical bond, have been presented in the literature.[13−20] They are based on the analysis of the electron pair density and take into account the influence of Pauli's exclusion principle which controls the delocalization (or localization) through a corresponding delocalization (or localization) of the Fermi-hole density. Thus, Bader et al. have shown[13] that the pairing of electrons is a consequence of the spatial localization of an electron of a given spin, as determined by a corresponding localization of its Fermi hole. They stablish an empirical correspondance between the localized charge concentration, defined by the negative of the Laplacian of the electron density and the number and arrangement of the localized electron pair domains defined by the VSEPR model of Gillespie.[14] They employ the Becke and Edgecombe electron localization function (ELF),[15] as a quantitative measure of the electron localization, and show that the topological structures that characterize the Laplacian of the electron density and the ELF are, in general, equivalent. These ideas have been used by Bader et al.[16] to show that the spatial distribution of the Fermi-hole density provides a quantitative basis for the concept of electron delocalization, commonly used throughout chemistry. Silvi and Savin[17] have studied the topology of the isosurfaces of the ELF to develop a nonempirical quantitative classification of the chemical bond based on Bader's classification of shared and closed-shell interactions and have applied it to a broad set of molecules, even to metallic bonds. Recently Cooper et al.[18] have employed *ab initio* SCF and spin-coupled wave functions to examine electron pair populations and the effective valencies generated from electron pair densities. They have found that the pair populations can be interpretated in terms of the contributions from various classical-VB Lewis structures. Also Ponec and Uhlick[19] have studied the role of electron pairing in chemical bonding, analyzing the electron pair fluctations in the bonding regions and showing that, in contrast to Bader and Stephen finding,[20] the Lewis electron-pair model is sufficiently accurate to provide a good basis for the description of molecular structures.

As was stated above, both, the VB theory and the Bader's theory have their own criterion for classifying the atomic interactions in the electron-pair bond as covalent (shared) or ionic (closed-shell). Nevertheless, these classifications do not necessarily come from the same paradigm, and each theory may render a different interpretation for identical bonds. What is clear is that the concept of "covalence-ionicity" is an important one in chemistry, which is related to the polarities and polarizabilities of electron-pair bonds. However, the fact that the degree of covalence (or ionicity) is not directly measurable introduces a source of considerable confusion in the literature, and to complicate matters even further, throughout chemistry, there is no single definition underlying the use of this concept. In the frame of the VB theory, several authors have dealt with the classification of the chemical bond as covalent or ionic. Among those, the works of Hiberty and Cooper[21] and Shaik, Hiberty, and collaborators[22] are worth mentioning in the context of this work. In the first of them,[21] the authors explore the quantitative relationship between the classical VB description of the chemical bond, eq 1, and that obtained from modern theories, as the generalized valence bond (GVB)[23] or spin-coupling (SC) methods,[6] where a Heitler−London type interaction with orbitals which are allowed to delocalized are considered. They prove that both descriptions are equivalent, by projecting a GVB or SC wave function onto a basis of classical VB structures built with purely local hybrids orbitals, this, in spite of the seemingly differences in languages between these two approaches. On the other hand, Shaik, Hiberty, and coworkers[22] use the resonance energy, defined as the energy stabilization of the principal resonance structure of eq 1 due to the interaction with all other resonance structures, in order to study the classification of the chemical bond. Based on this definition, they define a covalent bond as that having a bond energy close to the bond energy of the covalent structure and a small resonance energy, while an equivalent definition is given for an ionic bond. Those molecules with high resonance energy are classified within a third type of bonding called resonant. Thus, they report that most of the bonds having Fluor atoms belong to this last classification. Before continuing, it is important to remark that, like many concepts in chemistry, the definition of "covalence-ionicity" cannot be right or wrong; it can only be useful or not, and in some sense, it is a matter of taste choosing a particular definition for a particular problem. In our opinion, the notion of covalence-ionicity of the electron-pair bond is necessary in chemical education and theoretical chemistry, because it provides and exceptional framework, in terms of which we can organize patterns that are observed in the experiments. Despite all of this, it is not our intention in this manuscript to make unfruitful claims in favor of one picture of bonding or another. In this paper, we use, mainly for historical reasons, the terms "covalent-ionic" when we refer to the VB description and the terms "shared-closed shell" in the case of Bader theory. The central questions that we would like to address are as follows: how does the topology of the electron charge density depends on the wave function *ansatz* and how do the relative values of the mixing coefficients, C_1-C_3, affect the properties of the electron density at the BCP. We believe that this study may lead in the future to a critical reexamination

of the concepts associated with the electron-pair bond arising from various chemical structural theories. With these objectives in mind, in the next section we begin analyzing the properties of the electron charge density for the H−H and Li−H diatomic interactions and present some general properties of the electron density in the electron pair bond, when the bond goes from pure covalent to pure ionic. In section III, we show the results of GVB calculations and the analysis of the topology of the charge density for 15 different diatomic molecules at the optimized equilibrium possition: H−H, Li−Li, F−F, Na−Na, Cl−Cl, Li−H, B−H, F−H, Li−F, Na−H, Al−H, Cl−H, Na−F, Li−Cl, and Na−Cl. In this series we cover a wide range of covalent-ionic ratios both from VB theory and shared-closed shell bonds from the Bader's theory point of view. Thus, one can study how the topological properties of the charge density change with the type of the bonding properties. This set is a small samplings chosen in order to illustrate the relation between the characteristic features of the VB and Bader's theory. In section IV we study, in detail, the dependence with the internuclear distance of the VB description and the topological properties for the H−H and Li−H as archetypical examples of covalent and polar bonds, respectively, and the dependence with that distance of the other homonuclear diatomic bonds (Li−Li, F−F, Na−Na, and Cl−Cl), which present many exciting and interesting properties both in the VB's and Bader's theory's point of view.

II. The Topology of the Electron Charge Density as a Function of the Ionicity for the H−H and LI−H Bond

A. Numerical Results. In order to start exploring the answers to the questions stated before, in this section we have calculated the densities for two limiting situations, i.e., H_2 and LiH molecules. For the H−H interaction, we have used the so-called symmetric *ansatz,* in which the two ionic contributions have the same weight. This is represented by the wave function

$$\psi(H-H) = \Phi(HH) + \lambda_{ion}[\Phi(H^-H^+) + \Phi(H^+H^-)] \quad (3)$$

where λ_{ion} is the degree of ionicity. In the opposite extreme, we have chosen for the Li−H interaction the totally asymmetric *ansatz,* described by the wave function

$$\psi(Li-H) = \Phi(LiH) + \lambda_{ion}\Phi(Li^+H^-) \quad (4)$$

Equations 3 and 4 are not normalized. In the middle of these two extreme cases we may have intermediate situations, represented by *ansatz* with different weights of the structures A^-B^+ and A^+B^-. For simplicity, the densities have been calculated using s-Slater type orbitals (s-STO). The orbitals exponents were H1s−STO 1.19 and Li1s−STO 1.35, 2s−STO 0.65. Calculations of Figures 1 and 2 were made using experimental bond distances, H−H = 0.74 Å and Li−H = 1.60 Å. The wave functions Φ are the standard Heitler−London and ionic functions constructed from purely atomic s-STO.[1,24] In the next section we study in detail the form of the VB wave function.

Comparing the expressions for the densities obtained from the two previous *ansatz* wave functions, eqs 3 and 4, it can be observed that the density of a molecule can be split into three terms

$$\rho = \rho_{cov} + \rho_{res} + \rho_{ion} \quad (5)$$

where ρ_{cov}, is due to the covalent contribution only, ρ_{res} to the resonance between covalent and ionic structures, and ρ_{ion} comes from the ionic contributions only. The relative weights of each one of these terms depend on the value of λ_{ion} and reveal much of the variations in the charge distribution for different ionicities. Thus, when λ_{ion} is small, the principal contribution is ρ_{cov}. In a similar fashion, ρ_{ion} dominates for large ionicities, and for intermediate situations, each one of the terms presents a relatively important contribution. Based on this separation of ρ, we can talk about covalent, ionic, or resonating bonds. It is worth mentioning that similar description of the electron-pair bond was proposed by Shaik, Hiberty, and co-workers,[22] based on the concept of resonance energy instead on electron density. Here, in what follows, we examine the role of the resonance contribution in the variation of the topology of the electron density.

Figure la shows $\nabla^2\rho$ at the central BCP of the H_2 as a function of λ_{ion}. This result is very surprising, since the Laplacian does not increase, as we would expect, in going from shared interaction to closed-shell interactions. Instead, the Laplacian decreases for small ionicities, showing a minimum near $\lambda_{ion} = 0.6$. This minimum coincides with a maximum of $|\lambda_1|/\lambda_3$. From the Bader's point of view, the H−H bond presents a shared interaction behavior, no matter what the value of λ_{ion} is. The minimum in the Laplacian represents the ionicity at which the topological properties of the density present the most shared behavior. From the same figure, we can also notice that when the ionicity approaches extreme values (100% covalence, $\lambda_{ion} \rightarrow 0$, or 100% ionicity, $\lambda_{ion} \gg 1$), we cannot distinguish an ionic from a covalent bond, by using the density or any topological property thereof. Let us emphasize that, how it will be shown later, this behavior is independent of the fact that for the H−H interactions $\nabla^2\rho$ is negative for all ionicities, which is characteristic of shared type interactions. More insightful information, about the properties of the H−H symmetric *ansatz,* is obtained by analyzing the total density and its contribution at the BCP as a function of the ionicity, as displayed in Figure 1b. This figure shows that the total density has a maximum near $\lambda_{ion} = 0.6$. This maximum coincides with the crossing point of the covalent and ionic contribution, $\rho_{cov} = \rho_{ion}$, with a maximum in the resonance contribution, and with a minimum in the Laplacian of ρ. At the maximum of ρ, the contribution of their components are given approximately by $\rho_{cov} = 25\%$, $\rho_{res} = 50\%$, and $\rho_{ion} = 25\%$. These results lead us to think that the most shared type interaction corresponds with the most resonant type of bond in the H−H symmetric *ansatz*.

Figure 2 shows equivalent analysis for the Li−H interaction. From Figure 2a it can be seen how $\nabla^2\rho$ increases smoothly with the ionicity. This is just the expected behavior in going from shared to closed-shell interaction. Thus, in this case a large ionicity does imply a more closed-shell character of the bond. For the whole range of λ_{ion} in Li−H, the Laplacian is always larger than zero. Once more, additional information can be obtained by analyzing the total density and its contributions. Figure 2b shows that the total density does not reach a maximum (as could be expected from the Laplacian result), leveling off after $\lambda_{ion} = 1$. However, the crossing point of the covalent and ionic contributions again coincides with the maximum of the resonance contribution. Notice that due to the form of the *ansatz* function (4), the maximum of ρ_{res} at $\lambda_{ion} \approx 0.9$ does not imply the most shared character of the bond; instead, it could be thought that for that value of λ_{ion}, the topological properties of the electron charge density for this bond describe an intermediate situation between pure ionic and pure covalent behavior. Thus, for the asymmetric *ansatz*, the most resonant type bond shows topological properties intermediate with respect to the ones pertaining to the extremes values of λ_{ion}.

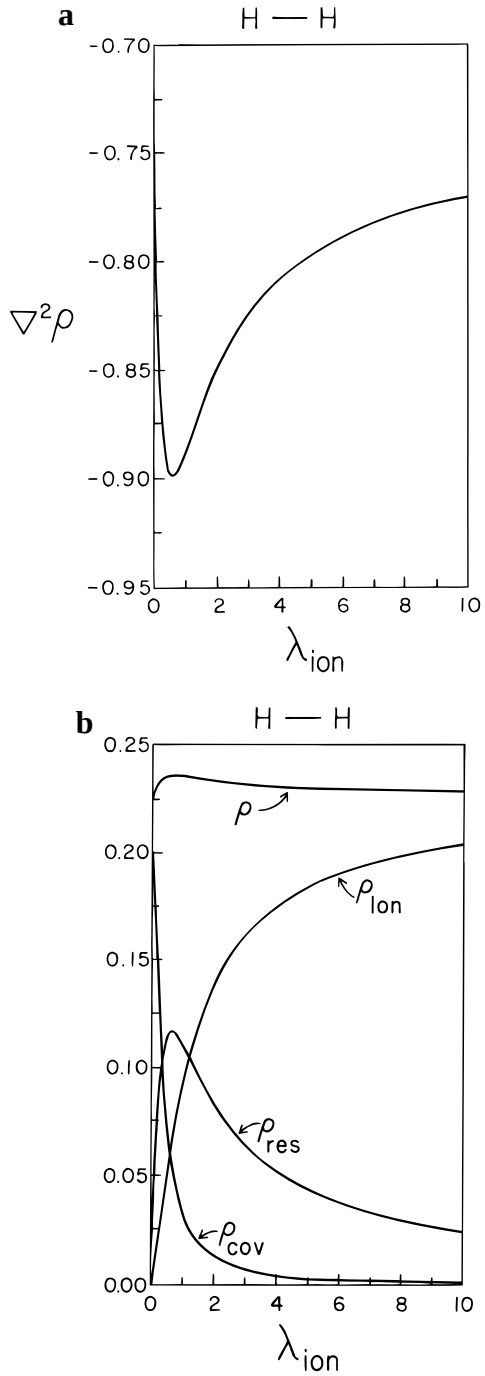

Figure 1. (a) Variation of $\nabla^2\rho$ at the BCP as a function of λ_{ion} for the H−H bond. (b) Variation of the electronic density and their components (defined in the text) at the BCP as a function of λ_{ion} for the H−H bond.

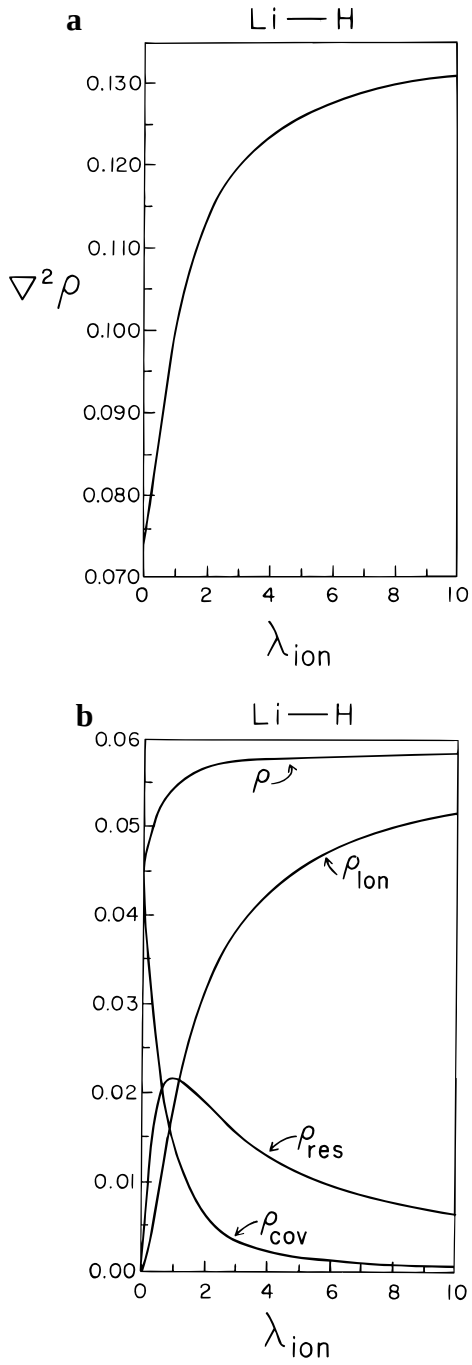

Figure 2. (a) Variation of $\nabla^2\rho$ at the BCP as a function of λ_{ion} for the Li−H bond. (b) Variation of the electronic density and their components (defined in the text) at the BCP as a function of λ_{ion} for the Li−H bond.

B. Analytical Results. The starting point for the discussion of the topology of the electron charge density in the electron-pair bond is the normalized form of the general wave function, eq 1,

$$\psi(A-B) = C_1\Phi(A\cdot\cdot B) + C_2\Phi(A^-B^+) + C_3\Phi(A^+B^-)$$

$$= N\{\Phi(A\cdot\cdot B) + \lambda_{i,1}\Phi(A^-B^+) + \lambda_{i,2}\Phi(A^+B^-)\} \quad (6)$$

where $\lambda_{i,1}$ and $\lambda_{i,2}$ are independent mixing coeficcients. For the case of the symmetric *ansatz*, $\lambda_{i,1} = \lambda_{i,2} = \lambda_{ion}$, and for the asymmetric *ansatz* $\lambda_{i,1} = \lambda_{ion}$ and $\lambda_{i,2} = 0$. The normalized valence bond structure functions are constructed from the product of two localized nonorthogonal hybrid orbitals between two atomic or molecular fragments centers, denoted by *a* and *b*, and a product of double occupied orthogonal *core* orbitals, denoted by {*core*}. These functions are given by

$$\Phi(A\cdot\cdot B) = \frac{\det(\{core\}a\bar{b}) + \det(\{core\}b\bar{a})}{\sqrt{2(1+S_{ab})}}$$

$$\Phi(A^-B^+) = \det(\{core\}a\bar{a})$$

$$\Phi(A^+B^-) = \det(\{core\}b\bar{b}) \quad (7)$$

here det represents a normalized Slater determinant and a bar over the letter denoting the hybrid orbital indicates spin-orbitals

with spin-down. The normalization constant of eq 6 is

$$N = \sqrt{\frac{1}{1+\lambda_{i,1}^2+\lambda_{i,2}^2+2(\lambda_{i,1}S_{12}+\lambda_{i,2}S_{13}+\lambda_{i,1}\lambda_{i,2}S_{23})}} \quad (8)$$

The elements of the overlap matrix between VB structures are

$$S_{12} = S_{13} = \frac{2S_{ab}}{\sqrt{2(1+S_{ab}^2)}}$$

$$S_{23} = S_{ab}^2 \quad (9)$$

and S_{ab} is the overlap integral between *a* and *b*.

In order to obtain the electron density corresponding to $\psi(A-B)$, the partition of eq 5 is employed, rendering the following results for the VB contributions to the total density:

$$\rho_{\mathrm{cov}} = N^2\left(\rho_{\mathrm{core}} + \frac{aa+2S_{ab}ab+bb}{1+S_{ab}^2}\right)$$

$$\rho_{\mathrm{res}} = N^2\left(\frac{4(\lambda_{i,1}+\lambda_{i,2})S_{ab}}{\sqrt{2(1+S_{ab}^2)}}\rho_{\mathrm{core}} + \frac{2(\lambda_{i,1}S_{ab}aa+(\lambda_{i,1}+\lambda_{i,2})ab+\lambda_{i,2}S_{ab}bb)}{\sqrt{2(1+S_{ab}^2)}}\right)$$

$$\rho_{\mathrm{ion}} + N^2((\lambda_{i,1}^2+\lambda_{i,2}^2+2\lambda_{i,1}\lambda_{i,2}S_{ab}^2)\rho_{\mathrm{core}} + 2(\lambda_{i,1}^2aa+2\lambda_{i,1}\lambda_{i,2}S_{ab}ab+\lambda_{i,2}^2bb)) \quad (10)$$

It is easy to show, that the contribution of the *core* density, ρ_{core}, to the total electron density, ρ, is constant, and the variation of the electron density with the VB independent coefficients, $\lambda_{i,1}$ and $\lambda_{i,2}$, only depends on the contribution of the nonorthogonal hybrid orbitals, *a* and *b*. Thus, as can be seen from eq 10, this density depends on three orbital products (*aa*, *bb*, and *ab*). The first two (*aa* and *bb*) increase the density on the atomic or molecular fragment center; however, the term *ab* increases the density on the bonding region; thus, it could be viewed as the resultant of the overall constructive interference between the localized fragment hybrid orbitals that allow the formation of the molecule. Notice that for the ρ_{cov} term, the contribution of these orbital products does not depend on the value of the VB coefficients, $\lambda_{i,1}$ and $\lambda_{i,2}$, for ρ_{res}, the contribution depends linearly with this coefficient, and for ρ_{ion}, the dependence is quadratic. In addition, the examination of the relative contribution of these three orbital products allows us to understand qualitatively the variations of $\nabla^2\rho$. For instance, taking into account that the term *ab* increases the density in the internuclear region, relative to the density of two noninteractive atoms, in general, this increment will cause a decrease in $\nabla^2\rho$ at the BCP. Accordingly, we expect a predominant shared type interaction when, at the BCP, *ab* is larger compared to the atomic or molecular fragments densities and a prevailing closed-shell type interaction when the atomic product, *aa* or *bb*, is the dominant contribution. We note that this behavior can be modified, if the geometric location of the BCP changes drastically with the ionicity, as in the assymmetric *ansatz*. From the previous discussion, it seems clear that the relative contributions of the terms *aa*, *bb*, and *ab* determine the topological properties of the density at the BCP. The relative weight of each of those terms depends on the ionicity in a manner that varies with the *ansatz* wave function. Thus, analyzing the contributions of each of those products, it is possible to understand the relationship between the valence bond theory and Bader's theory. On the other hand, a detailed analysis, based on the Laplacian instead of the density, would be more complicated; this is due to the complex dependence of $\nabla^2\rho$ on parameters as equilibrium distance, atomic basis set, orbital exponent, etc.

From the previous results, we can obtain some tendencies of the total density for the symmetric and the asymmetric *ansatz*. For the case of the symmetric *ansatz* ($\lambda_{i,1} = \lambda_{i,2} = \lambda_{\mathrm{ion}}$), it is readily shown that $\lim_{\lambda_{\mathrm{ion}}\to 0}\rho = \lim_{\lambda_{\mathrm{ion}}\to\infty}\rho$. This surprising result generalizes the one obtained numerically for the H_2 molecule, in the sense, that for a system described by a symmetric *ansatz* wave function, the density of a pure covalent bond ($\lambda_{\mathrm{ion}} \to 0$) is exactly the same as the density at infinity ionicity ($\lambda_{\mathrm{ion}} \to \infty$). Thus, it also allows the generalization of the conclusion previously drawn for this case: "we cannot distinguish an ionic from a covalent bond by using the density or any topological property thereof". For the assymmetric *ansatz*, this is not the case. Here we obtain that

$$\lim_{\lambda_{\mathrm{ion}}\to 0}\rho = \rho_{\mathrm{core}} + \frac{aa+2S_{ab}ab+bb}{1+S_{ab}^2}$$

$$\lim_{\lambda_{\mathrm{ion}}\to 0}\rho = \rho_{\mathrm{core}} + 2aa \quad (11)$$

in this case, the density at the BCP in an ionic bond ($\lambda_{\mathrm{ion}} \to \infty$) could be greater or smaller, relative to the covalent bond ($\lambda_{\mathrm{ion}} \to 0$), depending on the variation of the position of the critical point. However, due to the dependency on the factor *aa* in the ionic bond, we would expect that the Laplacian of the density increases with the ionicity.

If we do not consider the core density on each contribution of the electron charge density of eq 10, for the symmetric *ansatz* it can be shown that the maximum of the total charge density, ρ, and the maximum of the resonance contribution, ρ_{res}, occur at the same ionicity, which is given by

$$\lambda_{\mathrm{ion}}^R = \frac{1}{\sqrt{2(1+S_{ab}^2)}} \quad (12)$$

Moreover, for this ionicity it is also found that $\rho_{\mathrm{cov}} = \rho_{\mathrm{ion}}$. Thus, the point of maximum shared character of the electron charge density is located in general near $\lambda_{\mathrm{ion}}^R \to 0.6-0.70$. As we show in the next section, this value is very large compared with the variational results of λ_{ion} for some diatomic molecules. *In summary, in the symmetric ansatz the most shared interaction is characteristic of bonds with a highly resonating character.*

From the results of this section, we conclude that when the wave function *ansatz* describes a covalent and one ionic structure only, i.e., the totally asymetric *ansatz*, the transition from ionic to covalent VB description is analogous, in Bader's theory, to an increment in the direction to a shared type interaction. However, in the case of the symmetric *ansatz*, the increment in the shared type interaction is due to the resonance between ionic and covalent structures. These results lead us to think that, indeed, the topological properties of the electron density depend qualitatively on the type of the *ansatz* wave function employed to describe the system.

III. GVB Calculations

The properties of the electron charge density studied in the previous section are general results that come as a consequence

of the contruction of the wave function *ansatz*, without reference to any variational calculation. For example, the conclusion that the electronic charge density in the full ionic and the full covalent bond for the symmetric *ansatz* are the same is a general property of the wave function taken as an *ansatz* and is independent of the particular homopolar bond considered, i.e., H−H or F−F.

In this section, we report results of split valence with polarization and diffuse functions in heavy atoms and hydrogen, 6-31++G** (6-31++G(d,p)),[25] and triple ζ- with polarization and diffuse functions in heavy atoms and hydrogen, 6-311++G** (6-311++G(d,p)),[26] basis set, *ab initio* GVB[23] calculations on 15 diatomic molecules. The calculations have been performed using the *Gaussian-94* program.[27] The properties of the electronic charge density have been calculated from the AIM routine of *Gaussian-94*, developed by Cioslowski and co-workers.[28] Optimized equilibrium bond lengths have been used in the present study. In the GVB calculation, each single bond was treated as a GVB pair of σ symmetry, and the rest of the orbitals were kept doubly occupied. For homonuclear diatomic molecules, in order to localize the orbitals of the initial guess, the σ_g and σ_u irreducible representations are combined in the symmetry information used in the SCF calculation. This enables the orbitals to have lower symmetry than the full molecular point group, speeding up the convergence of the GVB function. The electronic densities are obtained from the natural orbitals of the GVB function. As it was mentioned in the introduction, Cooper et al.[4,5] pioneered the use of nonorthogonal spin-Coupling wave function[6] in the topological analysis of the electron density. With our level of calculation (GVB with a pair of nonorthogonal orbitals), we expect to obtain, at least, the correct qualitative behavior of the classical VB wave function and of the topology of the electron density. In general, our analysis will be aimed to discuss the general tendencies in the behavior of the VB wave function and the topology of the electron density rather than to concentrate on a quantitative detailed analysis of the results and in the comparison with similar calculations. At this point, let us mention that a more realiable accurate description of these VB wave functions can be obtained using spin-coupling[6] or VB wave functions with breathing orbitals, like the ones employed by Hiberty et al.[29] for F_2 and LiH.

The coefficients of covalent and ionic structures were obtained from the two localized GVB pair orbitals using the procedure described below. For diatomic molecules, the GVB wave function is written in terms of the GVB pair orbitals, ϕ_a and ϕ_b, as

$$\psi_{\mathrm{GVB}} = N\ \det|\{core\}\phi_a\phi_b(\alpha\beta - \beta\alpha)| = N\ \det|\{core\}(\phi_a\phi_b + \phi_b\phi_a)\alpha\beta| \quad (13)$$

where N is the normalization constant.

The GVB pair orbitals may be expressed in terms of the localized hybrid orbitals, a' and a'' on atom A and b' and b'' on atom B, through the following equation

$$\phi_a = N_a(a' + \delta_1 b'')$$
$$\phi_b = N_b(b' + \delta_2 a'') \quad (14)$$

where δ_1 and δ_2 are mixing parameters, whose absolute values are smaller than one. Then, the GVB wave function, ψ_{GVB}, can be written in terms of the localized hybrid orbitals as

$$\psi_{\mathrm{GVB}} = NN_aN_b\{\det|\{core\}a'b'(\alpha\beta - \beta\alpha)| + \delta_1\delta_2\ \det|\{core\}a''b''(\alpha\beta - \beta\alpha)| + \delta_2\ \det|\{core\}a'a''(\alpha\beta - \beta\alpha)| + \delta_1\ \det|\{core\}b'b''(\alpha\beta - \beta\alpha)|\}$$

$$\equiv C_{\mathrm{I}}^1\ \det|\{core\}a'b'(\alpha\beta - \beta\alpha)| + C_{\mathrm{I}}^2\ \det|\{core\}a''b''(\alpha\beta - \beta\alpha)| + C_{\mathrm{II}}\ \det|\{core\}a'a''(\alpha\beta - \beta\alpha)| + C_{\mathrm{III}}\ \det|\{core\}b'b''(\alpha\beta - \beta\alpha)| \quad (15)$$

Just as it happens with the wave function of eq 1, this GVB wave function can be split into three parts. The first two terms of eq 15 correspond to Heitler−London (covalent) type wave functions, in which the atoms exchange their electrons, and on average each center remains neutral. In the first term, this exchange occurs between the orbitals a' and b' with a weight equal to $C_{\mathrm{I}}^1 = NN_aN_b$, while the second covalent term involves a'' and b'' with a weight equal to $C_{\mathrm{I}}^2 = C_{\mathrm{I}}^1\delta_1\delta_2$. The third and fourth terms correspond to the ionic contributions. For the 15 diatomic molecules considered in this work, Table 1 shows the calculated bond length and the coefficients of the VB configuration functions of eq 15 computed by employing two different basis sets (6-31G** and 6-311G**). Table 1 also shows that, due to the usual small values of the mixing coefficients, δ_1 and δ_2, of eq 14, the value of C_{I}^1 in all cases is larger than C_{I}^2. Table 2 displays the properties of ρ at the BCP. Notice that the Li_2 molecule is not included in this table but is discussed elsewhere in this article.

From Table 1, it can be seen that for the homonuclear molecules, BH, NaH, and ClH, there is a prevalence of the contribution of the covalent structure over the ionic ones (coefficient C_{I}^1 larger than either C_{II} or C_{III}). On the other hand, for LiF, NaF, LiCl, and NaCl, the ionic contributions are the dominant ones (CI_{I} or C_{III} larger than C_{I}^1). A third kind of behavior can be noticed for LiH, FH, and AlH where both the covalent and ionic weights are important. The ionic character in homonuclear molecules decreases as Cl > F > H > Na ∼ Li, that is alkaline metals present lower ionicities than halogens; thus, we expect, in general, the ionicity in homonuclear bonds to be a reflection on the periodic trends of the elements.

Next, let us examine the results of Table 2. They indicate that, according to Bader's classification, the properties of the H_2, BH, FH, and ClH bonds correspond to shared type interactions, while the ones of the F_2, LiH, LiF, NaH, AlH, NaF, LiCl, and NaCl bonds correspond to closed shell type interactions. In general, it is satisfied that the value of $\nabla^2\rho$ is negative and large for the shared interaction and positive and small for the closed shell type. The homonuclear Na_2 and Cl_2 molecules present very small values for the Laplacian, −0.0020 for Na_2 and +0.0135 for Cl_2 (for the 6-311+G^* basis); thus, the internuclear distance at which the Laplacian changes sign ($\nabla^2\rho = 0$) at the BCP is close to their equilibrium geometry; therefore we expect these molecules to present intermediate character. However, from the values of $|\lambda_1|/\lambda_3$, we could classify Na_2 as having a shared type bond, with the largest $|\lambda_1|/\lambda_3$ among all the cases studied (including H_2), and Cl_2 as representative of a closed-shell character, with the largest value of $|\lambda_1|/\lambda_3$ for the series of studied molecules showing this kind of interaction.

Of all the examples listed in Tables 1 and Table 2, the homonuclear molecules are the ones that present the most interesting behaviors: the presence of non-nuclear attractor in Li_2, the closed-shell character of F_2 in spite of showing a typical

TABLE 1: Theoretical Bond Distance (R_e in Å), Coefficients of Canonical Valence Bond Structures (C_I^1, C_I^2, C_{II}, C_{III}), and Ionic Contribution to the Canonical Valence Bond Structures (λ_{ion}^{II}, λ_{ion}^{III})

bond	basis set	R_e	C_I^1	C_I^2	C_{II}	C_{III}	λ_{ion}^{II}	λ_{ion}^{III}
H−H	6-31++G**	0.7528	0.7701	0.0166	0.1325	0.1325	0.1684	0.1684
	6-311++G**	0.7565	0.7157	0.0268	0.1518	0.1518	0.2044	0.2044
Li−Li	6-31+G*	2.9764	0.9908	0.0049	0.0649	0.0649	0.0652	0.0652
	6-311+G*	2.9335	0.8997	0.0126	0.0991	0.0991	0.1086	0.1086
F−F	6-31+G*	1.5029	0.8430	0.0590	0.2618	0.2618	0.2902	0.2902
	6-311+G*	1.5157	0.8671	0.0569	0.2626	0.2626	0.2842	0.2842
Na−Na	6-31+G*	3.3987	0.7812	0.0058	0.1890	0.1890	0.2402	0.2402
	6-311+G*	3.3929	0.8886	0.0202	0.0961	0.0961	0.1057	0.1057
Cl−Cl	6-31+G*	2.0719	0.7375	0.0095	0.3149	0.3149	0.4216	0.4216
	6-311+G*	2.0748	0.7423	0.0103	0.3216	0.3216	0.4273	0.4273
Li−H	6-31++G**	1.6691	0.4888	0.0443	0.0509	0.5021	0.0955	0.9419
	6-311++G**	1.6371	0.6056	0.0329	0.0676	0.3526	0.1059	0.5522
B−H	6-31++G**	1.2502	0.6775	0.0739	0.1909	0.3519	0.2541	0.4683
	6-311++G**	1.2228	0.7062	0.0678	0.2073	0.2983	0.2678	0.3854
F−H	6-31++G**	0.9332	0.5288	0.0360	0.5458	0.0653	0.9663	0.1156
	6-311++G**	0.9174	0.5725	0.0538	0.4830	0.1051	0.7712	0.1678
Li−F	6-31+G*	1.5892	0.2721	0.0728	0.0423	0.8543	0.1226	2.4770
	6-311+G*	1.5797	0.2160	0.0530	0.0228	0.8675	0.0848	3.2249
Na−H	6-31++G**	1.9582	0.7833	0.0175	0.0729	0.2426	0.0910	0.3030
	6-311++G**	1.9472	0.6369	0.0281	0.0578	0.4013	0.0869	0.6034
Al−II	6-31++G**	1.6822	0.5807	0.1014	0.1449	0.5366	0.2124	0.7867
	6-311++G**	1.6808	0.5748	0.1002	0.14541	0.5104	0.2154	0.7561
Cl−HI	6-31++G**	1.2911	0.6863	0.0571	0.4049	0.1531	0.5447	0.2059
	6-311++G**	1.2884	0.6434	0.0576	0.3829	0.1512	0.5462	0.2157
Na−F	6-31+G*	1.9455	0.2188	0.0515	0.0170	0.9161	0.0781	3.2586
	6-311+G*	1.9454	0.1737	0.0513	0.0170	0.9161	0.0755	4.0716
Li−Cl	6-31+G*	2.0725	0.4675	0.0601	0.0406	1.0403	0.0770	1.9718
	6-311+G*	2.0408	0.3388	0.1233	0.0779	0.9600	0.1686	2.0755
Na−Cl	6-31+G*	2.4113	0.2173	0.0451	0.0164	0.9382	0.0625	3.5754
	6-311+G*	2.3964	0.3254	0.0483	0.0258	0.7874	0.0690	2.1070

TABLE 2: Topological Properties of the Electron Density at the Bond Critical Point

bond	basis set	ρ	$\nabla^2\rho$	$\lambda_1 = \lambda_2$	λ_3	$\lvert\lambda_1\rvert/\lambda_3$
H−H	6-31++G**	0.2371	−0.9378	−0.8366	0.7354	1.1376
	6-31++G**	0.2506	−0.9519	−0.8325	0.7131	1.1674
F−F	6-31+G*	0.1996	0.6639	−0.4472	1.5580	0.2870
	6-311+G*	0.1809	0.7440	−0.4091	1.5620	0.2619
Na−Na	6-31+G*	0.0065	−0.0023	−0.0014	0.0005	2.9189
	6-311+G*	0.0064	−0.0020	−0.0015	0.0009	1.5812
Cl−Cl	6-31+G*	0.1260	0.0330	−0.1597	0.3523	0.4533
	6-311+G*	0.1288	0.0135	−0.1629	0.3393	0.4801
Li−H	6-31++G**	0.0312	0.1285	−0.0431	0.2148	0.2007
	6-311++G**	0.0357	0.1459	−0.0519	0.2497	0.2078
B−H	6-31++G**	0.1818	−0.5812	−0.4312	0.2937	1.4682
	6-311++G**	0.1850	−0.4974	−0.4542	0.4110	1.1051
F−H	6-31++G**	0.3409	−2.0310	−2.0120	1.9920	1.0100
	6-311++G**	0.3770	−2.8470	−2.3340	1.8200	1.2800
Li−F	6-31+G*	0.0696	0.6862	−0.1609	1.0088	0.1596
	6-311+G*	0.0727	0.7118	−0.1666	1.0450	0.1599
Na−H	6-31++G**	0.0268	0.1101	−0.0284	0.1670	0.1703
	6-311++G**	0.0285	0.1119	−0.0319	0.1758	0.1818
Al−H	6-31++G**	0.0689	0.1811	−0.0899	0.3610	0.2490
	6-311++G**	0.0702	0.1853	−0.0922	0.3697	0.2494
Cl−H	6-31++G**	0.2287	−0.5935	−0.5609	0.5283	1.0617
	6-311++G**	0.2388	−0.5963	−0.5474	0.4986	1.0979
Na−F	6-31+G*	0.0492	0.4284	−0.0775	0.5834	0.1328
	6-311+G*	0.0501	0.4222	−0.0792	0.5806	0.1365
Li−Cl	6-31+G*	0.0379	0.2416	−0.0568	0.3552	0.1599
	6-311+G*	0.0447	0.2596	−0.0687	0.3970	0.1730
Na−Cl	6-31+G*	0.0298	0.1844	−0.0319	0.2482	0.1286
	6-311+G*	0.0329	0.1853	−0.0373	0.2599	0.1436

covalent interaction, and the small values of the Laplacian for Na_2 and Cl_2. For this reason in the next section we study their behavior from VB and Bader's point of view as function of the internuclear distance.

Next, it is interesting to compare the conclusions one can draw from Tables 1 and 2 employing VB and Bader's theory. Both theories agree that the H_2, Na_2, BH, and ClH bonds are covalent (shared) and that the LiF, NaF, LiCl, and NaCl bonds are of the ionic (closed shell) type. According to our best calculation, the 6-311G**, both the LiH and FH are mainly covalent bonds; this agrees well with the results given in Table 2 for the case of FH but not for the case of LiH. Also, F_2, Cl_2, and NaH are problematic, since from the VB point of view, these molecules are mainly covalent and from Bader's theory point of view are of the closed shell type. We note that the four cases with nonconcordance, F_2, Cl_2, LiH, and NaH, all present a dominant covalent character in a VB sense but a closed shell character in the Bader sense. This paradox will be explored in the next section.

It has been emphasized several times throughout the text that electron-pair bonding not only depends on the contributions of the covalent and the ionic functions but also on the extent of their mixing. However, there is not a simple way to obtain each of the contributions to the density at the BCP from the GVB wave functions describing the bonds. Thus, although we do not separate the calculated GVB wave function at the BCP in terms of covalent, ionic, and resonance contributions, in order to further discuss the results of Table 1, it would be desirable to get from this wave function a partition of the density, similar to the one given in eqs 5 and 10. To achieve this task, let us divide both sides of eq 15 by $C_I^1 + C_I^2$. Since $C_I^1 \gg C_I^2$, the coefficient of the first covalent term is approximately equal to one. Next, by neglecting the contribution of the second covalent term and defining a parameter λ_{ion}^J as

$$\lambda_{ion}^J = \frac{C_J}{C_I^1 + C_I^2}, \quad J = \text{II, III} \tag{16}$$

we obtain a wave function similar to the one given in eq 1. This fact allows us to perform an analysis, in terms of the limiting cases presented in section II. However, the ap-

TABLE 3: Total Energies (E in au), Coefficients of Canonical Valence Bond Structures (C_I^1, C_I^2, $C_{II} = C_{III}$), Overlap between Nonorthogonal GVB Pair Orbitals (S_{GVB}), and the Topological Properties Electron Density at the Bond Critical Point as Function of the H−H Bond Distance (R in Å)[a]

R	E	C_I^1	C_I^2	C_{II}	S_{GVB}	ρ	$\nabla^2\rho$	$\lvert\lambda_1\rvert/\lambda_3$
0.5	−1.074 091	0.6429	0.0431	0.1711	0.8649	0.4857	−3.997	2.4536
	−1.075 090	0.6014	0.0527	0.1852	0.8617	0.4851	−4.262	2.4828
0.6	−1.128 648	0.6748	0.0357	0.1637	0.8426	0.3772	−2.706	2.7564
	−1.129 565	0.6481	0.0406	0.1717	0.8391	0.3685	−2.212	1.5147
0.7	−1.147 701	0.6991	0.0311	0.1592	0.8168	0.2943	−1.630	1.8197
	−1.148 886	0.6958	0.0304	0.1572	0.8131	0.2863	−1.241	1.2171
0.8	−1.148 531	0.7166	0.0283	0.1572	0.7877	0.2312	−0.931	1.2646
	−1.150 052	0.7270	0.0249	0.1492	0.7838	0.2270	−0.798	1.1596
0.9	−1.139 962	0.7324	0.0260	0.1554	0.7555	0.1833	−0.537	1.0114
	−1.141 769	0.7447	0.0224	0.1467	0.7516	0.1826	−0.562	1.1794
1.0	−1.126 780	0.7489	0.0237	0.1527	0.7204	0.1465	−0.326	0.8913
	−1.128 782	0.7684	0.0208	0.1455	0.7167	0.1482	−0.401	1.1654
1.1	−1.111 675	0.7671	0.0213	0.1487	0.6825	0.1179	−0.209	0.8282
	−1.113 795	0.7733	0.0191	0.1434	0.6792	0.1208	−0.276	1.0671
1.2	−1.096 206	0.7870	0.0187	0.1431	0.6423	0.0953	−0.137	0.7819
	−1.098 389	0.7906	0.0171	0.1396	0.6393	0.0986	−0.177	0.9205
1.3	−1.081 304	0.8083	0.0161	0.1362	0.5999	0.0771	−0.087	0.7321
	−1.083 502	0.8101	0.0150	0.1340	0.5973	0.0804	−0.145	0.7775
1.4	−1.067 522	0.8303	0.0135	0.1279	0.5562	0.0625	−0.052	0.6724
	−1.069 688	0.8311	0.0128	0.1267	0.5539	0.0654	−0.053	0.6618
1.5	−1.055 161	0.8524	0.0111	0.1186	0.5116	0.0508	−0.026	0.6069
	−1.057 261	0.8526	0.0106	0.1180	0.5095	0.0532	−0.021	0.5789
2.0	−1.015 625	0.9428	0.0030	0.0679	0.3023	0.0185	+0.016	0.3528
	−1.017 494	0.9430	0.0029	0.0668	0.2998	0.0187	+0.015	0.3623
2.5	−1.002 069	0.9839	0.0006	0.0314	0.1562	0.0069	+0.010	0.2581
	−1.004 021	0.9839	0.0005	0.0296	0.1543	0.0067	+0.011	0.2569
3.0	−0.998 591	0.9965	0.0000	0.0013	0.0757	0.0026	+0.005	0.2147
	−1.000 599	0.9956	0.0000	0.0123	0.0749	0.0024	+0.006	0.1876

[a] At each bond distance, the first line corresponds to 6-31++G* basis set, and the second line to the 6-311++G** basis.

proximated character of this partition renders this discussion qualitative rather than quantitative. The results for λ_{ion}^J are shown in the last two columns of Table 1. From there, we can see that for the homonuclear molecules, $\lambda_{ion}^{II} = \lambda_{ion}^{III}$; therefore, they can be taken as examples of the symmetric *ansatz*. Additionally, since the values of the coefficients λ_{ion}^J are small compared to the typical values of λ_{ion}^R, given in eq 12 for the maximum resonance character of the bonds, we concluded that the covalent contribution, ρ_{cov}, is the most important one to the total density for the homonuclear molecules.. In analogous fashion, we can consider the LiF, NaF, LiCl, and NaCl bonds as very good examples of the asymmetric *ansatz*, since for all of these molecules one of the ionic contribution could be neglected respect to the other. Due to the large λ_{ion}^J coefficients, the ionic contribution to the density, ρ_{ion}, is the most important one in these molecules. The LiH, BH, FH, AlH, NaH, and ClH are not representative of the two previous *ansatz*. From the values of λ_{ion}^{II} and λ_{ion}^{III} given in Table 1, we expect that at the BCP, these bonds present a nonneglegible resonance contribution. We would also expect that the density in those bonds will not show either a dominant covalent or ionic character. Let us just mention, that in their analysis, Shaik and co-workers,[5] employing energy arguments, consider FH as a resonating bond, while they classify the LiH as covalent one. At this point, we freely admit that these results puzzle us, and we are carrying on some studies in order to formulate some plausible explanation for them.

IV. Dependence with the Internuclear Distance

In this section we explore how the values of the total energy, the overlap integral between the GVB nonorthogonals pairs orbitals ϕ_a and ϕ_b given in eq 14, the coefficients of the resonance structures in eq 15, and the topological properties of the electron charge density at the BCP change with the internuclear distance, R. Several representatives molecules, namely H_2, LiH, Li_2, F_2, Na_2, and Cl_2, are studied here.

In Table 3 we show the results obtained for the H_2. At the large distance limit, the energy is, as it should be, twice the ROHF energy of the hydrogen atom for the basis used here. The GVB wave function is mainly given by pure atomic orbitals centered on each of the hydrogens, i.e., the delocalization coefficient and the overlap integral, S_{GVB}, are close to zero, and values of the topological properties of ρ at BCP agree with a closed shell character, where the electronic density is mainly localized on each atom. When R decreases, the delocalization increases (as is reflected by the increase in C_I^2, C_{II}, and S_{GVB}), and the electronic density at the BCP grows monotonically. The Laplacian of the electronic density has an interesting behavior; it starts to increase from a value close to zero at large distances, until it reaches a small maximum (at about 2 Å), after which, it starts to decrease monotonically, showing then a typical shared interaction behavior (which can also be noticed from the values of $\lvert\lambda_1\rvert/\lambda_3$ displayed there). We think that the maximum at 2 Å is associated with the existance of a weak interaction (of van der Waals type) between the two hydrogen atoms. For larger values of R, the interaction between the atoms tends to disappear, and the values of ρ and $\nabla^2\rho$ go to zero. Notice that while the GVB wave function has a clear covalent character for all distances, the topological results may be interpreted as the system having a transition from a closed-shell behavior at large distances to a shared behavior at R about its equilibrium value. To understand this result, let us examine eq 10. There we can see that in the covalent density, ρ_{cov}, the term that depends on the pair orbital product ab is multiplied by overlap integral S_{ab}; thus, if a system has a covalent VB description and its overlap integral is small, it will show a closed-shell behavior. This may

TABLE 4: Total Energies (E in au), Coefficients of Canonical Valence Bond Structures (C_I^1, C_I^2, $C_{II} = C_{III}$), Overlap between Nonorthogonal GVB Pair Orbitals (S_{GVB}) and the Topological Properties Electron Density at the Bond Critical Point as Function of the Li−H Bond Distance (R in Å)[a]

R	E	C_I^1	C_I^2	C_{II}	C_{III}	S_{GVB}	ρ	$\nabla^2\rho$	$\lvert\lambda_1\rvert/\lambda_3$
1.5	−7.995 774	0.4277	0.0615	0.0627	0.5447	0.7651	0.042 96	+0.2135	0.2033
	−8.000 109	0.5449	0.0463	0.0751	0.4020	0.7575	0.045 31	+0.2200	0.2090
1.6	−7.998 513	0.4582	0.0532	0.0552	0.5241	0.7553	0.035 50	+0.1640	0.1990
	−8.002 224	0.5581	0.0390	0.0649	0.4031	0.7486	0.037 62	+0.1649	0.2028
1.7	−7.998 799	0.4879	0.0423	0.0478	0.5065	0.7432	0.029 67	+0.1252	0.1967
	−8.002 009	0.5703	0.0328	0.0559	0.4052	0.7375	0.031 59	+0.1235	0.2037
1.8	−7.997 369	0.5150	0.0337	0.0411	0.4917	0.7291	0.025 09	+0.0948	0.1968
	−8.000 176	0.5814	0.0276	0.0481	0.4075	0.7242	0.026 80	+0.0931	0.2061
1.9	−7.994 755	0.5389	0.0269	0.0353	0.4792	0.7132	0.021 46	+0.0713	0.1993
	−7.997 236	0.5920	0.0234	0.0416	0.4092	0.7091	0.022 94	+0.0701	0.2089
2.0	−7.991 343	0.5601	0.0218	0.0305	0.4687	0.6957	0.018 56	+0.0534	0.2039
	−7.993 564	0.6027	0.0199	0.0362	0.4100	0.6924	0.019 81	+0.0540	0.2126
2.1	−7.987 419	0.5791	0.0178	0.0265	0.4595	0.6768	0.016 21	+0.0399	0.2105
	−7.989 432	0.6742	0.0170	0.0319	0.4095	0.6742	0.017 24	+0.0414	0.2169
2.2	−7.983 192	0.5969	0.0147	0.0233	0.4512	0.6568	0.014 28	+0.0299	0.2186
	−7.985 042	0.6264	0.0146	0.0283	0.4075	0.6547	0.015 11	+0.0317	0.2224
2.3	−7.978 818	0.6142	0.0122	0.0206	0.4430	0.6356	0.012 68	+0.0224	0.2284
	−7.980 544	0.6340	0.0125	0.0253	0.4039	0.6340	0.013 34	+0.0240	0.2299
2.4	−7.974 418	0.6317	0.0102	0.0183	0.4344	0.6133	0.011 34	+0.0167	0.2394
	−7.976 052	0.6553	0.0107	0.0228	0.3987	0.6120	0.011 87	+0.0179	0.2402
2.5	−7.970 079	0.6499	0.0086	0.0164	0.4249	0.5898	0.010 21	+0.0124	0.2453
	−7.971 649	0.6721	0.0091	0.0206	0.3916	0.5888	0.010 64	+0.0129	0.2548
3.0	−7.951 281	0.7578	0.0033	0.0095	0.3541	0.4559	0.006 55	+0.0005	0.4562
	−7.952 764	0.7762	0.0040	0.0128	0.3286	0.4563	0.006 74	+0.0019	0.8042
3.5	−7.939 493	0.8719	0.0011	0.0054	0.2477	0.3097	0.004 04	−0.0003	0.5650
	−7.940 961	0.8842	0.0015	0.0083	0.2286	0.3103	0.003 93	+0.0010	0.4794
4.0	−7.933 885	0.9461	0.0004	0.0034	0.1482	0.1902	0.002 02	+0.0009	0.2997
	−7.935 343	0.9522	0.0006	0.0057	0.1351	0.1905	0.001 98	+0.0009	0.2899
4.5	−7.931 647	0.9797	0.0002	0.0021	0.0825	0.1127	0.000 97	+0.0008	0.2018
	−7.933 109	0.9819	0.0001	0.0042	0.0743	0.1129	0.000 97	+0.0008	0.2147
5.0	−7.930 820	0.9928	0.0000	0.0021	0.0446	0.0663	0.000 47	+0.0006	0.1630
	−7.932 285	0.9931	0.0000	0.0032	0.0040	0.0666	0.000 48	+0.0005	0.1754

[a] At each bond distance, the first line correspond to 6-31++G** basis set, and the second line to the 6-311++G** basis.

explain the results found in the last section, namely that F_2, Cl_2, LiH, and NaH show a dominant covalent character but not a shared type interaction behavior. This leads us to think that the overlap integral between the hybrid orbitals plays an important role in the topological properties of the electronic densities at the BCP and should be taken into account when these results are interpreted.

In Table 4, we display the results obtained for the LiH molecule. At large distances, the energy of the system is found to converge to a value identical to the sum of the atomic ROHF energies of lithium and hydrogen, and the GVB wave function is close to being purely covalent, with one of the orbitals totally localized over the atom of lithium and the other one over the hydrogen atom. When the distance decreases, the GVB pair orbitals become more delocalized, the contribution of the resonant structure with the negative charge on the hydrogen grows ($C_{II} < C_{III}$), and, as was mentioned in the last section, the covalent and ionic coefficients become comparably important ($C_I^1 \simeq C_{II}$). From the Bader's point of view, the LiH shows a closed-shell interaction behavior, with the electronic density at the BCP decreasing when R increases. For our best basis set (6-311++G**), $\nabla^2\rho$ becomes smaller when R grows, and $|\lambda_1|/\lambda_3$ displays a shallow minimum near the equilibrium position and a maximum at $R \sim 3$ Å. For the range of internuclear distances studied here, this behavior agrees well with the results reported by Cooper and Allan,[4] who related the maximum in $|\lambda_1|/\lambda_3$ with a change from an ionic to a covalent description in the SC wave function. Similarly to the H_2 case, we think that this maximum is related to the existence of a weak interaction, of the van der Waals type, between the Li and the H. For larger R, in agreement with those authors, we think that the covalent character should prevail. To further explore this point, let us consider the overlap integral. For $R > 3$ Å, the value of S_{GVB} decreases very rapidly, which is totally consistent with the closed shell character for these distances. On the other hand, when R decreases, the overlap integral starts to grow until it reaches a value close to 0.75 for which the wave function becomes very delocalized and the contribution of the ionic resonant structures becomes important. Again this ionic character corresponds to a closed-shell interaction of the molecule. We think that the FH and AlH molecules should have similar behavior like LiH, explaining in this way the results in section III.

The case of F_2 is also interesting; the results in Table 1 show that at the equilibrium distance ($R_e = 1.5$ Å) its bond could be classified as covalent, while from Table 2, one can classify the F_2 as having a closed-shell interaction. Again, looking for a plausible explanation to these results, we have studied how the GVB function and the topological properties at the BCP depend on the internuclear distance. We have found that for R smaller than 1.2 Å the bond interaction changes from closed-shell to shared (the Laplacian of the electronic density changes from +0.4835 at $R = 1.3$ Å to −0.0892 at $R = 1.2$ Å and −1.165 at $R = 1.1$ Å, while the relation $|\lambda_1|/\lambda_3$ goes from 0.330 at $R = 1.4$ Å to 0.857 at $R = 1.0$ Å). The changes in the values of the overlap integral (0.50355 at 1.5 Å, 0.73014 at 1.2 Å, and 0.79567 at 1.1 Å) show that both the overlap between pure atomic F orbitals and the delocalization of the GVB orbitals increase when R decreases; thus, as in the case of the H_2 molecule, the growth of S_{GVB} induces the shared character of the interaction to become evident. At the equilibrium distance the S_{GVB} is not big enough for the shared character to be the dominant one.

Table 2 shows that the Cl_2 molecule, at the equilibrium position, has a value for $\nabla^2\rho$ very close to zero, and Table 1 evidences an important contribution of the ionic structures in the GVB wave function; it is for this reason that we have decided to explore its behavior when the internuclear distance is changed. We have found that at distances larger than R_e, the Laplacian is always positive, displaying a small maximum at about 2.4 Å, which again may be interpreted as due to the existence of a weak interaction. The surprising results were observed at distances shorter than R_e. As could be anticipated, at distances close to the equilibrium position ($R \simeq 2.0$ Å) $\nabla^2\rho$ becomes negative; however, when R is further decreased, we observe the appearence of a non-nuclear attractor (more precisely in the range of R between 1.1 and 1.6 Å). In order to verify this result, we performed a calculation at $R = 1.5$ Å, employing the 6-311+G* basis at RHF, MP2, and CISD (configuration interaction with single and double substitution in the presence of frozen cores) levels, and always the non-nuclear attractor was found. As far as we know, this is the first time that this kind of behavior is reported for the Cl_2 molecule. At this point, we think it is essential to repeat this calculation with a more accurate basis set, to make sure, in this way, that this result is not an artifact of the basis set employed, as has happened with other cases previously reported in the literature.[11] At this moment this work is currently in progress in our laboratory.

One case where the existence of a non-nuclear attractor seems to be confirmed is the Li_2 molecule.[5,7−12] Some authors[10] claim that this attractor is present in the HOMO orbital of the Li_2 molecule, and they explain that from the nodal properties of the 2s-atomic orbital of Li. They predict that non-nuclear attractors might occur in long bonds of low polarity. Others have explained[12] that an electron−electron interaction which mixes the ground and appropriate excited electronic states can, under suitable conditions, cause instability of the ground state electron density at the midpoint between the nuclei of a homonuclear diatomic molecule to produce the midbond electron density maximum, that results in the appearance of the non-nuclear attractors. Despite all the effort put into this problem, there is not yet a widely accepted explanation for the presence of these attractors.

We have carried out calculations for Li_2 in a wide range of internuclear distances. For a large R (large than 3.6 Å for the 6-31+G* basis and 3.3 Å for the 6-311+G* basis) no non-nuclear attractors were found. The Laplacian shows a maximum at about 5.5 Å, in agreement with the results for other molecules mentioned before. Within a small range of shorter distances (3.4−3.5 Å for the 6-31+G* basis and 3.1−3.2 Å for the 6-311+G* basis), we have found the presence of two non-nuclear attractors, placed symmetrically about a BCP located in the middle of the bond.[9] For a range of R enclosing the equilibrium distance (between 2.2 and 3.3 Å for the 6-31+G* and 2.2−3.0 Å for the 6-311+G* basis) the system shows a non-nuclear attractor in the middle of the bond with two BCPs at each side of the central maximum. For distances shorter than 2.1 Å no non-nuclears attractors were found. It is worth mentioning that Cioslowski,[9] by employing catastrophe theory arguments, has reported this kind of behavior for the critical points of Li_2. Two more points deserve to be mentioned. As the internuclear distances decrease, the overlap integral grows until it reaches a maximum at about 2.1 Å, decreasing steadily afterward. We think, very much in agreement with Glaser et al.,[10] that due to the nodal properties of the 2s-valence electron density function of Li, there is a narrow range of internuclear distances where the overlap is sizable and out of that range it decreases noticeably. Secondly, we notice that for $R < 2.1$ Å, the values of the mixing parameters in the GVB pair orbitals are consistent with orbitals having a strong delocalization, with the wave function changing sign in the regions located over each Li nucleus.

Finally, we studied the molecule of Na_2. For this case, employing both of the basis mentioned before at the RHF, MP2, GVB, and CISD levels, we have not found non-nuclear attractors within the internuclear distance range studied here (2.0−4.01 Å). This is a controversial case; some authors have reported the existence of this kind of attractors,[8] while, later on, others[11] have shown that its presence is an artifact of the basis set employed and found that the non-nuclear attractor disappears when the basis is improved and the electron correlation level increased.

V. Summary

The results shown in this article lead us to think that the VB theory classification of the electronic pair bond as covalent and ionic and the Bader's classification of the atomic interactions as shared and closed-shell are complementary rather than equivalent. Moreover, from the values of the coefficients of the different resonant contributions to the GVB wave function, in many cases is not possible to infer the topological properties of the electronic density at the BCP. The reason for this may be understood if we think that the VB theory tries to explain the chemical bond as the result of the interaction of several resonant structures, which are characterized by atomic hybrid orbitals. Each of these structures is the result of the spin coupling in a singlet between the different hybrid orbitals, and it is this coupling which determines their covalent or ionic character. On the other hand, in the topological description of Bader's, all the properties are derived from the behavior of an observable, the electron density. Despite all this, some general results are to be mentioned: covalent structures (from the VB's point of view) with sizable overlap integral between hybrid orbitals present a shared type interactions. Also structures clearly ionic give a closed-shell interaction behavior. However, for polar sysytems, where the contribution of the ionic structures is important and the electronic density at the BCP is small, both theories may render conflicting results regarding the characterization of the electronic pair bond.

Acknowledgment. This research was supported by the Consejo de Desarrollo Científico, Humanístico y Tecnológico of the Universidad de Los Andes (CDCHT-ULA, Grant C-729-95). Computer support by CeCalCULA is gratefully acknowledged.

References and Notes

(1) Pauling, L. *The Nature of the Chemical Bond;* Cornell University Press: Ithaca, NY, 1939.

(2) Lewis, G. N. *J. Am. Chem. Soc.* **1916**, *38*, 762.

(3) Bader, R. F. W.; Essen, H. *J. Chem. Phys.* **1984**, *89*, 1943. Bader, R. F. W. *Atoms in Molecules: A Quantum Theory;* Oxford University Press: Oxford, 1990. Bader, R. F. W. *Chem. Rev.* **1991**, *91*, 893.

(4) Cooper, D. L.; Allan, N. L. *Chem. Phys. Lett.* **1988**, *150*, 287.

(5) Cooper, D. L. *Nature* **1990,** *346*, 796. Petch, B.; Cooper, D. L.; Gerratt, J.; Karadakov, P. B.; Raimondi, *M. J. Chem. Soc., Faraday Trans.* **1995**, *91*, 3751.

(6) Cooper, D. L.; Gerratt, J.; Raimondi, M. *Adv. Chem. Phys.* **1987**, *69*, 319. Cooper, D. L.; Gerratt, J.; Raimondi, M. *Chem. Rev.* **1991**, *85*, 92.

(7) Gatti, C.; Fantucci, P.; Pacchioni, G. *Theor. Chim. Acta* **1987**, *72*, 433.

(8) Cao, W. L.; Gatti, G.; MacDouall, P. J.; Bader, R. F. W. *Chem. Phys. Lett.* **1987**, *141*, 380.
(9) Cioslowski, J. *J. Phys. Chem.* **1990**, *94*, 5496.
(10) Glaser, R.; Waldron, R. F.; Wiberg, K. B. *J. Chem. Phys.* **1990**, *94*, 7357.
(11) Edgecombe, K. E.; Esquivel, R. O.; Smith, V. H., Jr.; Muller-Plathe, F. *J. Chem. Phys.* **1992**, *97*, 2593.
(12) Bersuker, G. I.; Peng, C.; Boggs, J. E. *J. Phys. Chem.* **1993**, *97*, 9323.
(13) Bader, R. F. W.; Johnson, S.; Tang, T.-H.; Popelier, P. L. A. *J. Phys. Chem.* **1996**, *100*, 15398.
(14) Bader, R. F. W.; Gillespie, R. J.; MacDougall, P. J. *J. Am. Chem. Soc.* **1988**, *110*, 7329. Gillespie, R. J. *Molecular Geometry;* VanNostrand Reinhold: London, 1972. Gillespie, R. J.; Hargittai, I. *The VSEPR Model of Molecular Geometry;* Allyn and Bacon: Boston, 1991.
(15) Becke, A. D.; Edgecombe, K. E. *J. Chem. Phys.* **1990**, *92*, 5397. Becke, A. D. *Int. J. Quantum Chem.* **1983**, *23*, 1925.
(16) Bader, R. F. W.; Streitwieser, A.; Neuhaus, A.; Laidig, K. E.; Speers, P. *J. Am. Chem. Soc.* **1996**, *118*, 4959.
(17) Silvi, B.; Savin, A. *Nature* **1994**, *371*, 683. Cooper, D. L. *Nature* **1994**, *371*, 651.
(18) Cooper, D. L.; Ponec, R.; Thorsteinsson, T.; Raos, G. *Int. J. Quantum Chem.* **1996**, *57*, 501. Ponec, R.; Strnad, M. *Int. J. Quantum Chem.* **1994**, *50*, 43.
(19) Ponec, R.; Uhlik, F. *J. Mol. Struct. (Theochem)* **1997**, *391*, 159.
(20) Bader, R. F. W.; Stephens, M. E. *J. Am. Chem. Soc.* **1975**, *97*, 7391.
(21) Hiberty, P. C.; Cooper, D. L. *J. Mol. Struc. (Theochem)* **1988**, *169*, 437.
(22) Sini, G.; Maitre, P.; Hiberty, P. C.; Shaik, S. *J. Mol. Struct. (Theochem)* **1991**, *229*, 163. Shaik, S.; Maitre, P.; Sini, G.; Hiberty, P. C. *J. Am. Chem. Soc.* **1992**, *114*, 7861.
(23) Bobrowicz, F. W.; Goddard, W. A. in *Method of Electronic Structure Theory;* Schaefer, H. F., Ed. Plenum: New York, 1977.
(24) Heitler, W.; London, F. *Z. Physsik* **1927**, *44*, 455. Slater, J. C. *Phys. Rev.* **1931**, *38*, 1190. Coulson, C. A. *Valence;* Oxford University Press: Oxford, 1961.
(25) Hehre, W. J.; Ditchfield, R.; Pople, J. A. *J. Chem. Phys.* **1972**, *56*, 2257. Hariharan, P. C.; Pople, J. A. *Theor. Chim. Acta* **1973**, *28*, 213. Cinkley, J. S.; Gordon, M. S.; DeFrees, D. J.; Pople, J. A. *J. Chem. Phys.* **1982**, *77*, 3654.
(26) Krishnan, R.; Binkley, J. S.; Seeger, R.; Pople, J. A. *J. Chem. Phys.* **1980**, *72*, 650.
(27) Gaussian 94 (Revision E.1); Frish, M. J.; Trucks, G. W.; Schlegel, H. B.; Gill, P. M. W.; Johnson, B. G.; Robb, M. A.; Cheeseman, J. R.; Keith, T.; Petersson, G. A.; Montgomery, J. A.; Raghvachari, K.; Al-Laham, M. A.; Zakrzewski, V. G.; Ortiz, J. V.; Foresman, J. B.; Cioslowski, J.; Stefanov, B. B.; Nanayakkara, A.; Challacombe, M.; Peng, C. Y.; Ayala, P. Y.; Chen, W.; Wong, M. W.; Andres, J. L.; Reploge, E. S.; Gompers, R.; Martin, R. L.; Fox, D. J.; Binkley, J. S.; Defrees, D. J.; Baker, J.; Stewart, J. P.; Head-Gordon, M.; Gonzalez, C.; Pople, J. A. Gaussian, Inc.: Pittsburgh, PA, 1995.
(28) Cioslowski, J.; Nanayakkara, A.; Challacombe, M. *Chem. Phys. Lett.*, **1993**, *203*, 137. Cioslowski, J.; Surjan, P. R. *J. Mol. Struct. (Theochem)* **1992**, *255*, 9.
(29) Hiberty, P. C.; Humbel, S.; Byrman, C. P.; van Lenthe, J. H. *J. Chem. Phys.* **1994**, *101*, 5969. Hiberty, P. C. *J. Mol. Struct. (Theochem)* **1997**, *398*, 35.